Mon. Not. R. Astron. Soc. **276,** 1148–1154 (1995)

Modelling the activity of 2060 Chiron

Dina Prialnik,[1] Noah Brosch[2] and Drora Ianovici[2]

[1] *Department of Geophysics and Planetary Sciences, Raymond and Beverly Sackler Faculty of Exact Sciences, Tel Aviv University, Tel Aviv 69978, Israel*

[2] *The Wise Observatory and the School of Physics and Astronomy, Raymond and Beverly Sackler Faculty of Exact Sciences, Tel Aviv University, Tel Aviv 69978, Israel*

Accepted 1995 May 11. Received 1995 May 5; in original form 1995 February 6

ABSTRACT

Model calculations of the evolution of 2060 Chiron explain the observed activity pattern as being the result of a delayed thermal pulse in a porous matrix composed of dust and of amorphous water ice, which contains a small amount of trapped CO. Crystallization of the amorphous ice, accompanied by the release of the occluded gas, constitutes the source of activity. Many different combinations of parameters are tested. A composition dominated by crystalline water ice or ices of CO or CO_2 is ruled out. The model that best reproduces the temperatures inferred from IR observations at several heliocentric distances, as well as the rates of mass ejection, is obtained by assuming a relatively low effective surface emissivity.

Key words: comets: general – comets: individual: 2060 Chiron – minor planets, asteroids.

1 INTRODUCTION

Chiron (1977UB = 2060 Chiron) is a strange body in the Solar system, in that it develops at random intervals a coma, which appears to be composed of neutrally coloured material devoid of emission lines. For some years it was classed as asteroid, but the episodic coma formation caused it to be classed with the comets. Since its 1977 discovery by Kowal, its orbit was followed and extrapolated backward and forward in time (e.g., by Stern 1989 and by Hahn & Bailey 1990). Its orbit appears chaotic, and results of simulations do not agree; some claim that Chiron is a young object in the inner Solar system, while others find a higher probability that it resided even closer to the Sun, being a short-period comet for the last 100 000 yr.

Marcialis & Buratti (1993) summarized the brightness variations of Chiron during the last 20 yr. By using archive observations, they found that since its discovery, and even before, the object darkened until about 1985. From 1985 a steady brightening took place until 1989, and then a further darkening was observed. The excursion in brightness spanned more than 1.5 mag (a dimming by a factor of 5 or more). This evolution in brightness is contrary to the heliocentric distance; Chiron will only reach perihelion in 1996 in its 50-yr orbit, and it dims as it approaches the Sun. The first episode of coma formation occurred in 1978, during the middle of the decline in brightness. The second episode, in 1989, coincided with the maximal brightness. The coma reached vast dimensions during this event – a diameter of about 130 000 km by the beginning of 1990 February and 230 000 km by the end of that month. During this strong outburst, Bus et al. (1991) detected extended emission of CN λ3875 Å out to ~50 000 km from the nucleus. From this, they calculated a steady-state rate of mass loss of 3.7×10^{25} s^{-1} HCN molecules (assumed to be the parent molecule of CN).

The nucleus of Chiron is characterized by a fast rotation rate (21 304.7 ± 0.2 s ≃ 5.92 h; Bus et al. 1989). The coma, whenever it develops, is probably not gravitationally bound to the nucleus (Luu & Jewitt 1990; Meech & Belton 1990). If a steady-state coma exists, it presumably represents only a small fraction of the coma observed at episodes of activity. Fulle (1994) modelled the coma as it appeared in images obtained by West (1991), and derived a mass-loss rate of 20 ± 10 kg s^{-1} between 1987 and 1990, which is dominated by 100-μm grains.

Luu & Jewitt (1993) showed that, in addition to the long-term trends, the episodic brightening at the end of the 1980s, and the periodic variations connected with the rotation of the nucleus, Chiron also exhibits a random variation in brightness. This is already apparent on archive plates. Even near aphelion, in the late 1960s and early 1970s, Chiron underwent a major outburst in which it brightened by 1.5 mag for longer than 8 yr (Bus et al. 1993). Assuming a geometric albedo of 0.1, its diameter would be ~200 km; a lower, Halley-type albedo of 0.04 would imply a larger diameter of about 300 km. A non-detection at 800 μm puts an upper limit of 300 km to the diameter (Jewitt & Luu 1992). An

occultation of a star by Chiron in 1993 yielded the first lower limit to the diameter of the body: 166 km (Buie et al. 1993). An observation from a different site provided the tantalizing evidence of a short, stubby jet in existence at the time of the observation. An additional occultation in 1994 indicated a similar feature; namely, the existence of a narrow (few km) jet-like feature that reached a few hundred km from the nucleus. The observations of Chiron by Campins et al. (1994) yielded for the first time a number of temperature and radius estimates of the body.

In the following sections, we describe a series of models calculated with the comet nucleus evolution code developed by Mekler, Prialnik & Podolak (1990) and Prialnik (1992), which allows for porosity and gas flow, in an attempt to reproduce at least some of the characteristics of Chiron deduced from observations. In Section 2, the method of computation, basic assumptions and parameters are briefly described; the results of numerical computation for different parameter combinations are given in Section 3. The model which best reproduces the observed properties of Chiron is described in more detail in Section 4. A short discussion and conclusions follow in Section 5.

2 METHOD OF COMPUTATION AND INITIAL PARAMETERS

Evolutionary models of Chiron were calculated using a numerical code that solves the equations of mass and energy conservation for a spherically symmetric (fast-rotating) porous nucleus in a given orbit around the Sun (for details, see Prialnik 1992). The fast-rotator approximation is well-justified for Chiron. The nucleus is assumed to be composed of dust, amorphous and crystalline water ice, water vapour, and other volatiles (such as CO, CO_2, etc.), which may be frozen, free, or occluded in the amorphous ice. The code takes into account sublimation from the surface and from the pore walls, crystallization of the amorphous ice, which releases heat and liberates a large fraction of the trapped gases (according to the experimental studies of Bar-Nun et al. 1985, 1987), and transport of volatiles through the porous interior, which affects the thermal structure through advection and recondensation.

Two different sets of input parameters are required for constructing an evolutionary model of a comet nucleus. One set relates to the general characteristics of the particular comet one attempts to model: orbit parameters, radius (R), emissivity (ϵ) and albedo (A). The published orbit of Chiron was used, with an eccentricity of 0.38. We assumed a radius of 148 km (the average of values given by Jewitt & Luu 1992), an albedo of 0.04 (similar to Halley's), and several values for the emissivity. Recent estimates suggest a smaller nuclear radius for Chiron (~ 83 km, Buie et al. 1993; 90 km, Campins et al. 1994), but this should not affect the model results significantly, since we find that only an outer layer of a few hundred metres ($\ll R$) at most could be involved in Chiron's activity and thermal evolution. A smaller radius also implies a slightly higher albedo, around 0.1, but adoption of this value instead of 0.04 would not affect the results by more than a few per cent. The second set of parameters is more problematic: it involves the detailed composition of the nucleus (i.e., the mass fractions of the different components), its density (or porosity) and typical pore size, and the initial temperature distribution, all of which are unknown and have to be guessed.

The initial configuration was assumed to be homogeneous with a uniform temperature of 60 K and a pore size of 10 μm, and the porosity was taken to be 1/3 (unless otherwise stated). The composition of the model was varied, and many different evolutionary sequences were computed. Constraints on the possible structure and composition were obtained from observations of the activity of Chiron – in particular, data directly related to the nucleus. The aim was to reproduce the surface temperatures measured in the IR: ~ 100 K at 15.8 au from the Sun, ~ 122 K at 10.0 au, $126(^{+11}_{-6})$ K at 8.9 au, and $137(^{+14}_{-9})$ K at 8.8 au (Campins et al. 1994), and to derive a rate of mass ejection consistent with those derived from observations – in particular, the upper limit obtained for the CO production rate at ~ 9 au from the Sun: $(6.5\text{–}15)\times 10^{27}$ s^{-1} (Womack & Stern 1994).

3 RESULTS OF EVOLUTIONARY CALCULATIONS

The initial parameters and main results obtained for each evolutionary sequence are summarized in Table 1. We started by computing baseline models of simple composition: pure crystalline ice (model 1 in Table 1) and pure amorphous ice (model 2), adopting an effective emissivity of 0.5. The models were evolved until a steady state was reached, where the variation of the surface temperature and molecular fluxes with heliocentric distance, shown in Fig. 1, did not change from one orbit to the next. The crystalline ice model reached a peak temperature of ~ 103 K (shortly post-perihelion) and the amorphous ice one reached a higher peak temperature of ~ 110 K (due to its lower thermal conductivity), both significantly lower than the measured temperatures. We note that, in spite of the relatively low surface temperatures, and contrary to the assumption of Stern (1989), crystallization of the amorphous ice did occur, although at a slow rate (roughly 1 m yr^{-1}). According to Schmitt et al. (1989), the time-scale for crystallization as a function of temperature T is given by $\tau_{a-c} = 9.5\times 10^{-14}\exp(5370/T)$ s. For $T\sim 100$ it is ~ 600 yr, while for $T\sim 110$ it drops to ~ 5 yr. As the evolutionary time-scale of Chiron in (or approximately around) its present orbit is of the order of hundreds of years (several orbits), crystallization is expected to become important as a heat and gas source whenever the surface temperature exceeds ~ 100 K. A third model was computed for a mixture of 50 per cent crystalline ice and 50 per cent dust (by mass). This model reached a slightly higher peak surface temperature than the pure ice one, ~ 104 K. Both crystalline ice models showed a large difference in surface flux between the distances of 14 and 10 au. This should correspond to a marked increase in the activity of Chiron between these two epochs, which has not been observed.

The results changed drastically, if a relatively small amount of CO_2 ice was added to Chiron's composition. This is shown by our fourth model with an initial composition of 50 per cent crystalline ice, 5 per cent CO_2 and 45 per cent dust (by mass). The effect of the CO_2 ice is to keep the surface temperature almost constant, between 81 and 82 K, which is the sublimation temperature of CO_2. The surface flux, predominated by CO_2 is also almost constant, at a rather high value. This model too is incompatible with

Table 1. Models for Chiron.

Model	ϵ	ρ	H_2O	CO_2	f_{CO}	Dust	T_P	T_A	$\log(F_P)$	$\log(F_A)$
1	0.5	0.60	1.00(c)	-	-	-	102.5	81.5	20.75	14.09
2	0.5	0.60	1.00(a)	-	-	-	109.6	91.6	22.43	17.67
1A	0.9	0.60	1.00(c)	-	-	-	89.7	70.4	17.07	8.97
2A	0.9	0.60	1.00(a)	-	-	-	96.1	66.2	19.02	6.57
3	0.5	0.896	0.50(c)	-	-	0.50	103.6	81.0	20.83	13.70
4	0.5	0.88	0.50(c)	0.05	-	0.45	82.1	81.0	28.35(CO_2)	28.14(CO_2)
5	0.5	0.60	1.00(a)	-	0.001	-	130.2	120.0	28.04(CO)	28.11(CO)
5A	0.9	0.60	1.00(a)	-	0.001	-	96.0	66.2	25.23(CO)	21.45(CO)
6	0.5	0.994	0.40(a)	-	0.001	0.60	106.0	83.6	27.97(CO)	27.54(CO)
7	0.5	0.901	0.399(a)	0.001	0.001	0.60	98.3	84.5	26.53(CO_2)	25.61(CO_2)
7A	0.9	0.901	0.399(a)	0.001	0.001	0.60	92.7	82.4	26.22(CO_2)	25.30(CO_2)
8	0.25	0.373	0.40(a)	-	0.001	0.60	131.4	97.0	26.38(CO)	26.32(CO)

Notes to Table 1.

(1) The headings of the table are ϵ – the effective emissivity, ρ – the bulk density; H_2O – the various initial mass fractions of water ice, in amorphous (a) or crystalline (c) form; CO_2 – carbon dioxide ice; f_{CO} – the fraction of carbon monoxide trapped in the amorphous ice; Dust – the mass fraction of dust; all are used as input parameters.

(2) The initial temperature is 60 K for all models, the pore size is 10 μm, and the porosity is 1/3 (except in the last model, labelled 8, for which the porosity is 3/4).

(3) The results are the perihelion and aphelion surface temperatures (K), T_P and T_A, respectively, and the logarithm of the perihelion and aphelion molecular flux (molecule s^{-1}), only for the maximal flux among the different species (as marked).

observations. The effect of the assumed emissivity on the pure ice models is illustrated in Fig. 2, where the orbital variation of the surface temperature is shown for $\epsilon = 0.9$, and in Table 1 (models 1A and 2A): a higher emissivity obviously lowers the surface temperature. In the case of the amorphous ice, the lower temperatures prevent crystallization almost completely. As a result, the temperature range is stretched, since there is no internal heat source to compensate for cooling at large heliocentric distances. The conclusion we draw from this first group of models is that crystalline ice can be ruled out as the main component of Chiron – in particular, if it is mixed with more volatile ices, even in small mass fractions.

The next group of models involved gas-laden amorphous water ice; the trapped gas was assumed to be CO, constituting a fixed fraction of 0.1 per cent (by mass) of the ice. Several compositions were adopted, as shown in Table 1 (models 5 to 7) and Fig. 3. The effect of a high emissivity was tested again for two of the models (models 5A and 7A). A complex model involving amorphous ice, trapped gas, CO_2 ice and dust (Fig. 4, model 7 in Table 1) shows that the surface temperature is still dominated by the presence of CO_2 ice, even if its abundance is very small (less than 1 per cent). Hence species more volatile than H_2O may be ruled out altogether, at least for the outer layers of Chiron. The only model, so far, for which the surface temperatures came reasonably close to the measured ones (at small heliocentric distances) and produced a CO flux compatible with the observationally derived upper limit, was that of pure amorphous ice with trapped gas, for an emissivity of 0.5. Such a composition is, however, unrealistic, as dust constitutes a large fraction of the mass of any comet. In addition, the temperature range obtained for this model was much too narrow, resulting in too high temperatures at large heliocentric distances. In spite of these discrepancies, it became clear that gas-laden amorphous ice should be a major ingredient in Chiron's composition. The additional appeal of such a composition is the possibility of obtaining outbursts on different time-scales due to spurts of crystallization and gas release and possible fracturing of the ice, phenomena that cannot be simulated by a spherically symmetric model, but are bound to occur in real comets (Prialnik & Bar-Nun 1990, 1992; Prialnik et al. 1994).

4 A MODEL FOR CHIRON

In order to increase the surface temperatures and, at the same time, the temperature difference between perihelion and aphelion, for a reasonable gas-laden amorphous ice and dust mixture, we increased the porosity so as to lower the effective thermal conductivity (and thus decreased the density to ~ 0.4 g cm^{-3}, consistent with current estimates for

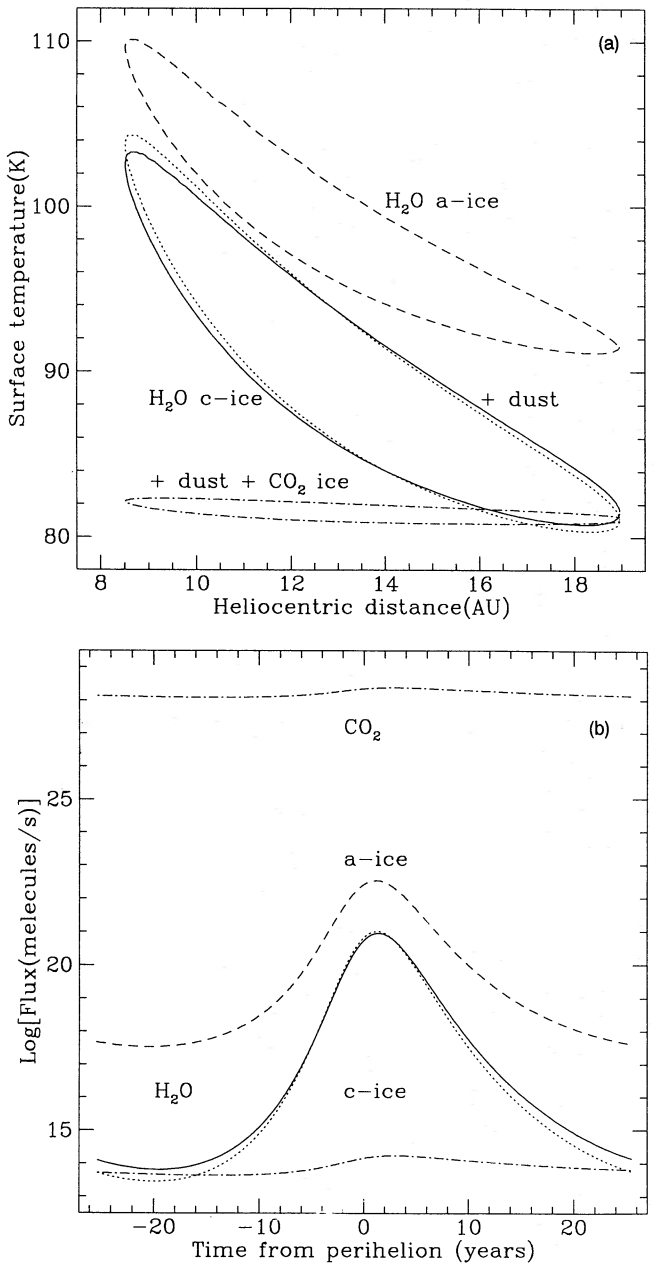

Figure 1. Orbital variation of (a) surface temperature and (b) molecular fluxes for different models (as given in Table 1): 1 – pure crystalline ice (solid line); 2 – pure amorphous ice (dashed line); 3 – crystalline ice and dust (dotted line); and 4 – crystalline ice, dust, and CO_2 ice (dash–dotted line).

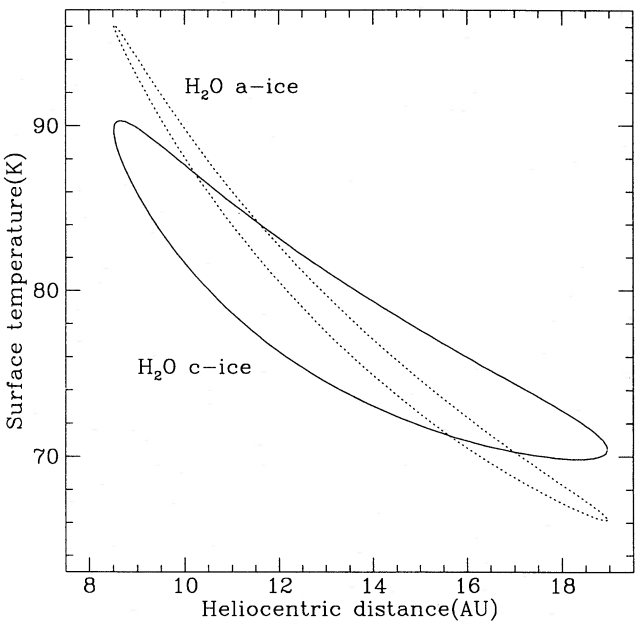

Figure 2. Orbital variation of surface temperature with $\epsilon = 0.9$ for pure ice models: 1A – crystalline ice (solid line); and 2A – amorphous ice (dotted line).

comets, e.g. Rickman 1989), and we lowered the emissivity. The value of ϵ was chosen on the basis of simple models of surface energy balance (without conduction to or from the interior):

$$(1-A)L_\odot/16\pi d_H^2 = \epsilon\sigma T^4 + \dot{Z}H, \quad (1)$$

where d_H is the heliocentric distance, σ is the Stefan–Boltzmann constant, $\dot{Z}$ is the sublimation rate of ice, and H is the latent heat of sublimation (the second term on the right-hand side is, in fact, negligible compared with the first, along the entire orbit of Chiron). Solving for $T(d_H)$, for different values of ϵ, we obtained a fair agreement with the measured temperatures for $\epsilon = 0.25$. We therefore adopted this value in the model calculations.

For a composition of 60 per cent dust and 40 per cent amorphous ice, occluding a fraction 0.001 of CO, we were thus able to obtain a model (labelled 8 in Table 1) that agrees remarkably well with the observational data, as shown in Fig. 5. A higher CO production rate was obtained by increasing the fraction of trapped CO, to 0.01 (with no significant effect on other characteristics); nevertheless, the production rate increased by less than a factor of 10, as the average rate of crystallization slowed down to some extent.

We find that crystallization does not occur continuously, but in spurts that start at large heliocentric distances (see also Prialnik & Bar-Nun 1990), close to aphelion. As a rule, the CO production rate decreases slightly as the model comet approaches the Sun from aphelion. This should explain the puzzling fading of Chiron between 1970 and 1985 (i.e., from ~ 18 to ~ 14 au). We expect dust (or dust and ice) grains to be carried with the CO flux. The rate of mass loss by gas is roughly between 5 and 50 kg s^{-1}. The mass of the ejected dust should be comparable to that of the gas. Two of the particular cases shown in Fig. 5(b) correspond to continuous, moderate outgassing typical of 'quiet' periods, and a third shows the activity shortly after the onset of a crystallization spurt.

Spectrophotometric observations of Chiron at a heliocentric distance of 11.26 au (Bus et al. 1991) detected extended CN emission. Assuming HCN to be the parent molecule of CN, and assuming CN to be 10 times less abundant than CO (as indicated by the detailed observations of P/Halley), the CN flux could be interpreted either as a result of continuous emission, equivalent to a CO production rate of 4×10^{26} molecule s^{-1}, or as a result of a recent outburst, implying a HCN production rate of 1.4×10^{27}

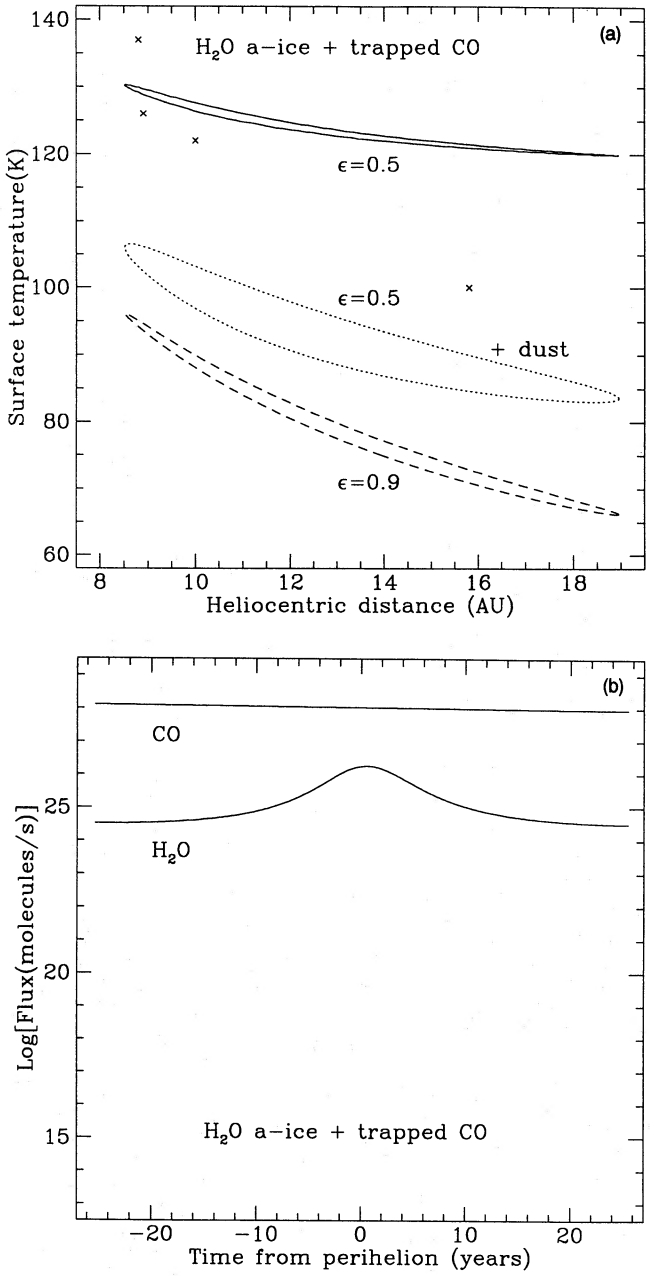

Figure 3. Orbital variation of (a) surface temperature for gas-laden amorphous ice models, as given in Table 1: 5 (solid line), 5A (dashed line) and 6 (dotted line). Temperature estimates from observations are indicated by crosses. (b) Molecular fluxes for model 5.

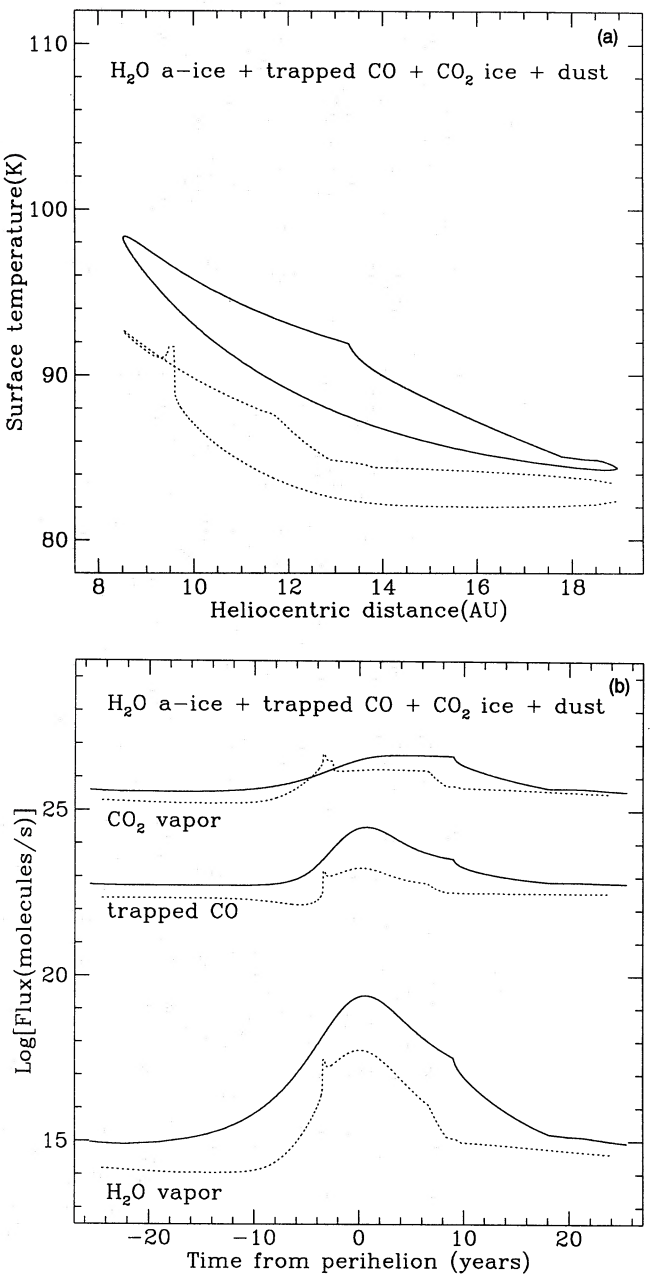

Figure 4. Orbital variation of (a) surface temperature and (b) molecular fluxes for a model including gas-laden amorphous ice, dust and CO_2 ice, for two emissivity values: model 7 – $\epsilon = 0.5$ (solid line) and model 7A – $\epsilon = 0.9$ (dotted line).

molecule s^{-1} and a CO production rate of $\sim 1.4 \times 10^{28}$ molecule s^{-1}. The CO emission was suggested to result from sublimation from an exposed limited surface area, and was invoked as the driving force of the HCN emission. Our models produce the required CO emission rates, as shown in Fig. 5(b), resulting from release of trapped gas. If the ratio of CO to HCN trapped in the amorphous ice is 10:1, the observed CN emission is accounted for, without having to resort to ad hoc assumptions regarding dragging of HCN molecules with the CO flux, resulting from sublimation from restricted surface areas. Both interpretations for CN emission – continuous outgassing or outburst – are compatible with our models; they require different circumstances (initial parameters and history). The CO flux at 9 au is consistent with the upper limit recently derived from observations by Womack & Stern (1994), as shown in Fig. 5(b).

For how long could such a level of activity be maintained, given that the history of Chiron is uncertain? A rough estimate may be obtained by assuming an average continuous CO output, say, $F_{CO} \approx 10^{27}$ molecule s^{-1}. Thus, for a given radius R, mass fraction of ice X_{ice} and fraction of occluded gas f_{CO}, the period of activity t_{CO} should be

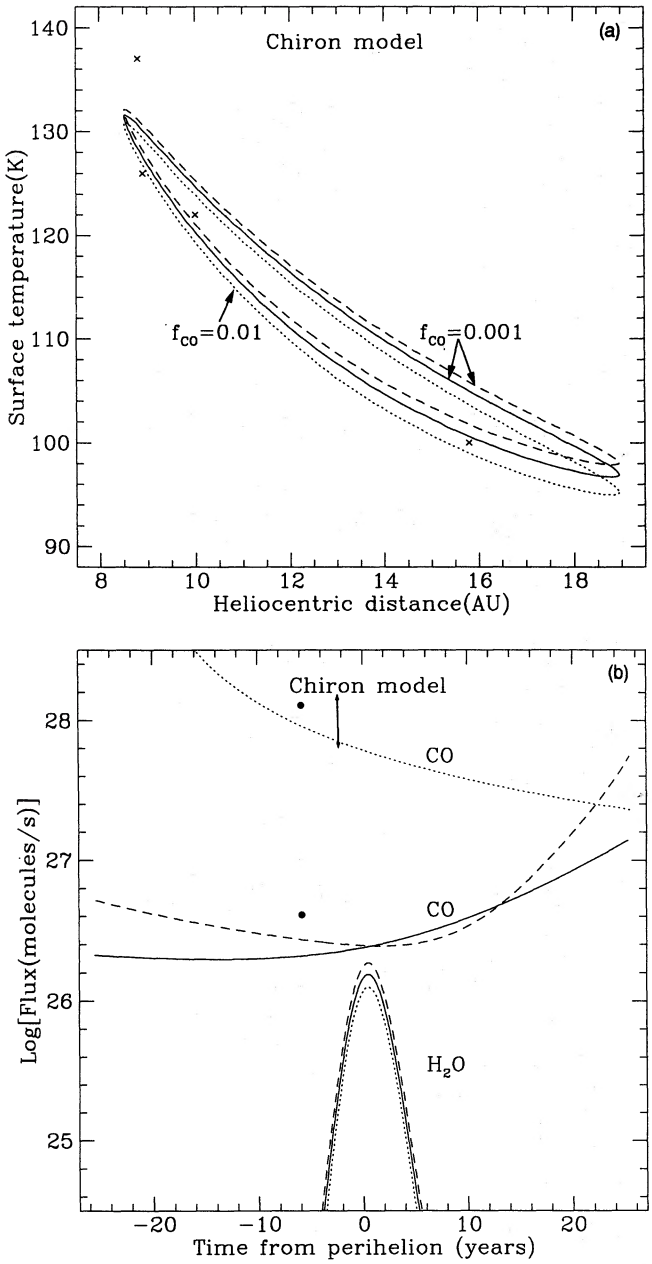

Figure 5. Orbital variation of (a) surface temperature and of (b) molecular fluxes for acceptable Chiron models: 40 per cent (by mass) amorphous ice including a fraction f_{CO} of trapped CO (as indicated) and 60 per cent dust, for the 20th orbit (solid and dotted lines) and for the 10th orbit (dashed lines). Temperature estimates from observations (omitting error bars) are indicated by crosses. Production rates inferred from CN detection are shown by dots. An observationally estimated upper limit for the CO flux is also indicated.

$$t_{CO} \approx \frac{4\pi R^3 \rho X_{ice} f_{CO}}{3 F_{CO} m_{CO}} \approx 10^9 \left(\frac{R}{100\ \mathrm{km}}\right)^3 X_{ice} f_{CO}\ \mathrm{yr}, \qquad (2)$$

where m_{CO} is the molecular mass, and a bulk density $\rho \approx 0.4$ g cm^{-3} has been assumed. This is ample time, even for low values of X_{ice}, f_{CO} or R, and hence no constraints can be imposed on Chiron's age (in its present, or a similar, orbit) from these considerations.

Table 2. Variations on Chiron's model.

ϵ	p	dust:ice	T_{min}	T_{max}	Comments
0.25	0.75	3:2	96	133	acceptable
0.50	0.75	3:2	80	110	T_{mim}, T_{max} too low
0.25	0.33	3:2	98	125	T_{max} too low
0.25	0.75	2:3	110	137	T_{min} too high

The next step in our investigation was to test the sensitivity of the model to the assumed parameters, in order to estimate how stringent is our composition and structure determination in the indirect manner that we have outlined. Several models were computed, each differing from the basic one in only one parameter. The results are summarized in Table 2. It turns out that changing the value of each one of the assumed parameters spoils the agreement with observations considerably. Our prediction is, therefore, that Chiron's effective surface emissivity (the emissivity averaged over the entire surface) is low. This may have implications for the surface structure and composition; for example, it may indicate that the grains producing the thermal continuum radiation are small. We note that the activity of our model is governed by the interior properties (the source of CO is at a depth of tens of hundreds of metres below the surface); it depends on surface properties only through A (mostly in the visible) and ϵ (in the IR). Hence considerable freedom is left for the choice of surface composition and structure. We should also point out that, in spite of the sustained activity, the surface may be considerably aged; it is not rejuvenated, as in comets that come regularly closer to the Sun and lose an outer layer of ice on each orbit.

Of course, testing the effect of each parameter separately might not be enough; one may ask what would happen if two parameter values were changed, and so on; there are still numerous possibilities that have not been explored. Nevertheless, we have found one viable model that should be put to the test in future observations. More importantly, perhaps, we have ruled out a large part of the free parameter space, and this should help in constructing future, more detailed or accurate models of Chiron.

5 DISCUSSION AND CONCLUSIONS

Our models indicate that a configuration of gas-laden amorphous water ice and dust reproduces many of the observed characteristics of Chiron – in particular, the estimated surface (colour) temperatures at different points of the orbit by Campins et al. (1994). The mass-loss rate from our preferred model is $\sim 10^{26}$–10^{27} molecule s^{-1} $\simeq$ 5–50 kg s^{-1}. This is comparable to the mass-loss rate through large dust grains calculated by Fulle (1994) for the late 1980s appearance of Chiron, and compatible with the rate inferred by Meech & Belton (1990), but higher than the rates of Luu & Jewitt (1990). The CO production rates are compatible with the rates inferred from observations by Bus et al. (1991) and by Womack & Stern (1994). Gas release from the ice

matrix can occur anywhere in the orbit, through spurts that start at large heliocentric distance.

The surface temperature of our one-dimensional models is uniform. In reality, however, Chiron's surface may be far from isothermal in spite of its rapid spin, since the spin axis is likely to be close to the orbital plane. In this case, one side would be exposed to insolation for long periods of time, while the other would be left in the dark. The temperature of the heated side would then be higher than that obtained here. The difference may be roughly estimated on the basis of equation (1), by multiplying the right-hand side by a factor of $\alpha < 1$, representing the fractional surface of the 'summer-side' of the comet. The increase in temperature would amount to a factor of the order of $\alpha^{-1/4}$. Even for $\alpha \sim 0.5$ the temperature would increase by only ~ 15 per cent, which is of the same order as the observational errors. It is, in fact, more instructive to reverse the argument. The coefficient $\alpha\epsilon$ may be regarded as an effectively reduced emissivity. Our conclusion that an unusually low average emissivity is required so as to reproduce Chiron's characteristics may be taken to mean that the surface temperature is non-uniform, so that a considerable fraction of the surface area has a negligible thermal emission, i.e. relatively low temperatures. This would indicate that the spin axis is indeed close to the orbital plane; we may further speculate that a very low effective emissivity could be interpreted in terms of a non-spherical body with a particular orientation of the spin-axis with respect to its longer axis.

It should be mentioned that seasonal effects fade away at depths of a few metres, the skin-depth of the nucleus. Hence one-dimensional models where the activity originates at large depths below the surface (as in our case) should be considered quite reliable.

Another question is whether our models – spanning a sequence of a few tens of revolutions in a fixed orbit – can represent the present-day state of the comet. Chiron's chaotic orbit (due to its proximity to Saturn and Uranus) makes it impossible to infer its long-term dynamical evolution accurately. Contrary to estimates that this is an unusually new comet, recently arrived from the Oort cloud (Hartmann et al. 1990), there is statistical evidence that Chiron may be on an evolutionary path from the outer part toward the inner part of the Solar system, similar to the paths of short-period comets (Scholl 1979), or even that it may have spent at long as 1 Myr in its present kind of orbit, with possible shorter intervals of higher activity in orbits closer to the Sun (Hahn & Bailey 1990). We have shown that the activity of Chiron resulting from our models could be maintained at the same level and pattern for a very long period of time, up to a few million years. Hence, whatever the evolution of Chiron's orbit has been, our models are still roughly representing the present-day state of the comet, in so far as the activity and surface properties are concerned. By the same token, they cannot impose constraints on the time Chiron has spent in its present orbit.

ACKNOWLEDGMENTS

We thank Morris Podolak and Yuri Mekler for helpful discussions, and Hans Rickman for valuable comments and suggestions. This work was supported by the Adler Fund for Space Research, received through the Commission for Basic Research of the Israeli Academy of Sciences and Humanities.

REFERENCES

Bar-Nun A., Herman O., Laufer D., Rappaport M. L., 1985, Icarus, 63, 317
Bar-Nun A., Dror J., Kochavi E., Laufer D., 1987, Phys. Rev., 35, 2427
Buie M. W. et al., 1993, IAU Circ. 5898
Bus S. J., Bowell E., Harris A. W., Hewitt A. V., 1989, Icarus, 77, 223
Bus S. J., A'Hearn M. F., Schleicher D. G., Bowell E., 1991, Sci., 251, 774
Bus S. J., Bowell E. L. G., Stern S. A., A'Hearn M. F., 1993, in Huebner W. F., Keller H. U., Jewitt D., Klinger J., West R., eds, Workshop on the activity of distant comets. Southwest Research Institute, San Antonio, Texas, p. 41
Campins H., Telesco C., Osip D., Rieke G., Rieke M., Schulz B., 1994, AJ, 108, 2318
Fulle M., 1994, A&A, 282, 980
Hahn G., Bailey M. E., 1990, Nat, 348, 132
Hartman W. K., Tholen D. J., Meech K. J., Cruikshank D. P., 1990, Icarus, 83, 1
Jewitt D. C., Luu J. X., 1992, AJ, 104, 398
Luu J. X., Jewitt D. C., 1990, AJ, 100, 913
Luu J. X., Jewitt D. C., 1993, in Huebner W. F., Keller H. U., Jewitt D., Klinger J., West R., eds, Workshop on the activity of distant comets. Southwest Research Institute, San Antonio, Texas, p. 44
Marcialis R. L., Buratti B. J., 1993, Icarus, 104, 234
Meech K. J., Belton M. J. S., 1990, AJ, 100, 1323
Mekler Y., Prialnik D., Podolak M., 1990, ApJ, 356, 682
Prialnik D., 1992, ApJ, 388, 196
Prialnik D., Bar-Nun A., 1990, ApJ, 363, 274
Prialnik D., Bar-Nun A., 1992, A&A, 258, L9
Prialnik D., Egozi U., Bar-Nun A., Podolak M., Greenzweig Y., 1994, Icarus, 106, 499
Rickman H., 1989, Adv. Space Res., 9, 59
Schmitt B. S., Espinasse S., Grim R. J. A., Greenberg J. M., Klinger J., 1989, ESA-SP, 302, 65
Scholl H., 1979, Icarus, 40, 345
Stern S. A., 1989, PASP, 101, 126
West R. M., 1991, A&A, 241, 635
Womack M. P., Stern S. A., 1994, IAU Circ. 5957